High-resolution projections of mean and extreme precipitation over Spain using the WRF model (2070–2099 versus 1970–1999)

D. Argüeso,[1,2] J. M. Hidalgo-Muñoz,[1] S. R. Gámiz-Fortis,[1] M. J. Esteban-Parra,[1] and Y. Castro-Díez[1]

Received 23 December 2011; revised 18 May 2012; accepted 21 May 2012; published 28 June 2012.

[1] A set of eight simulations at high spatial resolution (10 km) were performed with WRF to generate future projections of mean and extreme precipitation over Spain. The model was driven with two GCMs (ECHAM5 and CCSM3.0) under the conditions of three SRES emissions scenarios (B1, A1B and A2) which amounts to six future (2070–2099) climate simulations. Two present (1970–1999) climate simulations forced by the same GCMs were previously completed and were used as a baseline to allow for comparison and quantify the changes. The annual and seasonal precipitation means were examined to elucidate how global warming will manifest in the future precipitation climatic means. The distribution of precipitation in different-intensity events and the percentiles were calculated to further describe the nature of the changes. Additionally, a number of extreme indices were explored to determine changes in the low frequency events and the persistency of specific conditions. The results indicate that Spain might be exposed to a substantial decrease in annual precipitation that range between −18% and −42% depending on the simulation, with a particularly severe reduction during the summer, between −32% and −72%. These changes are generally caused by less light-to-moderate events, which leads to a displacement of the probability density function toward higher values. Namely, future climate might be characterized by less precipitation but more concentrated in extreme events, although their occurrence in absolute terms might not vary. The projections also suggest that, by the end of the century, the wet periods might be shorter and the dry spells significantly longer.

Citation: Argüeso, D., J. M. Hidalgo-Muñoz, S. R. Gámiz-Fortis, M. J. Esteban-Parra, and Y. Castro-Díez (2012), High-resolution projections of mean and extreme precipitation over Spain using the WRF model (2070–2099 versus 1970–1999), *J. Geophys. Res.*, *117*, D12108, doi:10.1029/2011JD017399.

1. Introduction

[2] The arise of Regional Climate Models (RCMs), and more generally the downscaling techniques, has been motivated by the necessity to bridge the gap between the regional scales and current spatial resolution in General Circulation Models (GCMs), which is strongly constrained by computational resources.

[3] In spite of their limitations [*Giorgi*, 2006a; *Laprise*, 2008; *Rummukainen*, 2010], RCMs have been revealed to be a valuable tool to overcome the problems derived from the GCMs coarseness and to provide climate information that is crucial to nature and human life. This specially applies to heterogeneous and complex-terrain regions such as the Iberian Peninsula (IP), where topography exerts strong influence on the climate. As a result of their finer resolution, RCMs are likely to resolve fine-scale characteristics that are know to affect the climate, such as the land-use or the vegetation [*Ge et al.*, 2007; *Hong et al.*, 2009; *Sánchez et al.*, 2007], and describe topographical features that might alter the local circulation [*Giorgi*, 2006a].

[4] The benefit of high-resolution simulations is particularly significant in the study of variables that are essentially local and unevenly distributed [*Rummukainen*, 2010] because they are governed by processes that are more likely to be correctly represented at higher spatial resolution, such as precipitation. Indeed, RCMs generally improve rainfall frequency and spatial distribution with respect to boundary conditions data [*Bukovsky and Karoly*, 2011; *Caldwell et al.*, 2009; *Leung and Qian*, 2009; *Salathé et al.*, 2008; *Laprise*, 2008]. Additionally, bearing in mind the local nature of some extreme events, especially in areas where precipitation has a significant convective component, the use of RCMs constitutes an additional advantage since the spatial resolution increase contributes to

[1]Department of Applied Physics, Faculty of Sciences, Universidad de Granada, Granada, Spain.
[2]Climate Change Research Centre, University of New South Wales, Sydney, New South Wales, Australia.

Corresponding author: D. Argüeso, Department of Applied Physics, Faculty of Sciences, University of Granada, Campus de Fuentenueva s/n, ES-18071 Granada, Spain. (dab@ugr.es)

0148-0227/12/2011JD017399

Table 1. Acronyms for the Future WRF Simulations

	ECHAM5	CCSM
B1 scenario	WEB1	WCB1
A1B scenario	WEA1B	WCA1B
A2 scenario	WEA2	WCA2

better simulate the distribution and magnitude of these events [*Bell et al.*, 2004; *Frei et al.*, 2003; *Giorgi*, 2006a].

[5] However, there are regions that still represent a challenge to RCMs and the IP is certainly one of them [*Herrera et al.*, 2010], as evidenced by some unsatisfactory results obtained over southern Europe and the IP [*Boberg et al.*, 2010; *Kjellström et al.*, 2010]. The present-climate precipitation in the IP is characterized by important inter-annual variability [*Rodriguez-Puebla et al.*, 2008] and a marked annual cycle modulated by the seasonal displacement of the Azores high-pressure system, which already leads to significant intra-annual variability [*Serrano et al.*, 2008]. The IP is also distinguished by its particularly complex topography composed by steep and narrow mountain ridges that distribute precipitation across the Peninsula generating a pronounced spatial variability, with large number of climate types such as Atlantic, Mediterranean, alpine or semi-arid over a relatively small region [*Castro et al.*, 2007; *Esteban-Parra et al.*, 1998].

[6] Furthermore, the Mediterranean area - and consequently Spain - has been identified as one of the hot spots in the global projections [*Giorgi*, 2006b], potentially being a region where climate change could manifest particularly severely in the future. Indeed, most GCMs suggest that the IP is expected to be among the most affected regions by precipitation decreases in the future [*Christensen et al.*, 2007a]. Therefore, the generation of high-resolution climate change information is especially meaningful over this region considering its peculiarities and its future vulnerability.

[7] The assessment of precipitation changes at regional scales over the Iberian Peninsula has been previously approached within the framework of two international projects that represent a milestone in regional climate modeling in Europe: PRUDENCE [*Christensen et al.*, 2007b] and ENSEMBLES [*van der Linden and Mitchell*, 2009]. Some authors [*Beniston et al.*, 2007; *Gao et al.*, 2006; *Gao and Giorgi*, 2008; *Giorgi and Lionello*, 2008; *Sánchez et al.*, 2011] have also examined the projected changes in precipitation over this region using RCMs. However, this paper contributes to the existing information on precipitation changes over Spain by supplying with a set of projections at an unprecedented spatial resolution (10 km), spanning a 30-year climate period and forced by two GCMs under the conditions of three different emission scenarios. In addition, the simulations have been completed with the Weather Research and Forecasting (WRF) modeling system which was not included in any of the aforementioned projects and studies.

2. Model Setup

[8] The Weather Research and Forecasting Model v.3.1.1 [*Skamarock et al.*, 2008] was adopted to complete a set of simulations covering 30-year periods: 2 for present climate (1970–1999) and 6 for future climate (2070–2099). The simulations were actually divided into decadal integrations to optimize the computational resources and a 7-month spin-up was selected. Despite the fact that very-deep soil variables (moisture and temperature) might need longer periods to actually reach equilibrium at some locations, surface and top-layer variables require much shorter spin-up periods. Indeed, although some studies used spin-up periods of one year or more [*Steiner et al.*, 2009; *Christensen et al.*, 2007b], most of the regional climate studies limited their spin-up periods to a few months [*Pfeiffer and Zängl*, 2010; *Evans and McCabe*, 2010; *Fernández et al.*, 2007; *Liang et al.*, 2008].

[9] Two different GCMs were employed to provide the large-scale information: the NCAR CCSM3.0 (run *e*) [*Collins et al.*, 2006] and the Max Planck Institute ECHAM5 model (run01) [*Roeckner et al.*, 2003] . Besides the two GCMs, three different emissions scenarios (B1, A1B and A2) were selected, which amounted to six future climate simulations (Table 1), to take into consideration the uncertainty associated to future greenhouse gases (GHGs) concentration in the atmosphere.

[10] A 10-km resolution domain containing 135 by 135 grid points and covering the entire IP (36°N–43.5°N, 9.5°W–3.3°E) was one-way nested in a coarser 30-km resolution domain centered in the IP and composed of 130 (W-E) by 120 (N-S) grid points. The location and extension of the domains are shown in Figure 1. The vertical is divided in 35 levels that extend up to 50 hPa. A weak spectral nudging [*von Storch et al.*, 2000] using a wave number 3 (only spatial scales larger than ~1300 km) was adopted in order to reduce the outputs dependency on the domains design and preserve the consistency between the GCM large scale and the regional scale defined by the RCM. The spectral nudging was only applied to the coarse domain (no nudging was selected for the inner one) and only above the Planetary Boundary Layer (PBL). All input variables were nudged except humidity, to avoid competition with convective schemes.

[11] A configuration of the physics schemes suited to reproduce the Iberian climate [*Argüeso et al.*, 2011] was chosen: Betts-Miller-Janjic [*Betts and Miller*, 1986; *Janjic*, 1990, 1994] for cumulus, Asymmetric Convective Model version 2 [*Pleim*, 2007] for the PBL, the WSM3 [*Hong et al.*, 2004] for the microphysics, the Noah Land-Surface Model [*Chen and Dudhia*, 2001] and the CAM3.0 radiation model [*Collins et al.*, 2004]. The CAM3.0 model allows for modification of the GHGs concentrations depending on the emission scenario. The modified version of the model clWRF [*Fita and Fernández*, 2010] was employed to that purpose.

3. Model Evaluation

[12] The generation of future climate projections requires the evaluation of the model in order to determine the confidence of the results. The performance of the model with this configuration was evaluated by *Argüeso et al.* [2012] using Spain02 [*Herrera et al.*, 2012], a daily gridded observational dataset that covers the entire present-climate period. A brief summary of the model validation is here provided and further details could be found in *Argüeso et al.* [2012]. The model suitability to generate high-resolution projections of climate change over Spain was assessed and, despite some non-negligible deviations with respect to observations in certain regions, it was shown that WRF adequately captures most of the features of Spanish precipitation. Indeed, the major

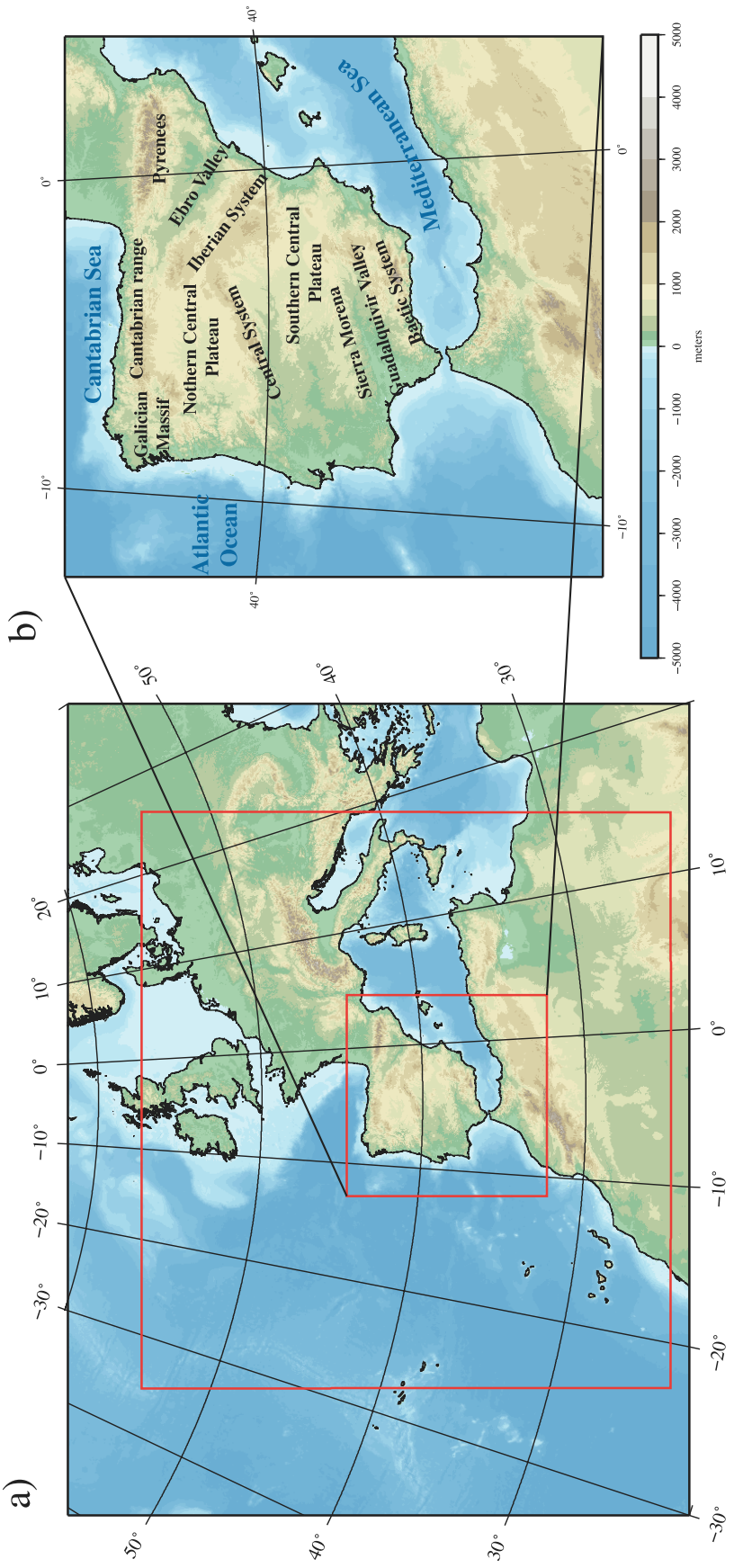

Figure 1. (a) Location of the WRF domains (red lines). (b) Main topographical features of the Iberian Peninsula.

advantage of using WRF is its ability to differentiate the climate regimes and incorporate the effect of small topographical features. It also shows a good skill with respect to the spatial distribution of extreme events, particularly when driven by reanalysis or ECHAM5. In general, precipitation is fairly well captured at all timescales, although some substantial seasonal biases were observed over particular regions, principally during the spring. It must be also stated that those deficiencies were highly induced by the large-scale structures forced by the boundary conditions. The model also tends to generate too much light precipitation, which is a feature common to other atmospheric models [*Denis et al.*, 2002; *Rosenberg et al.*, 2010; *Herrera et al.*, 2010]. Along the year, WRF overestimates rainfall during the first months, whereas it is able to reproduce remarkably well the precipitation during the last half of the year.

4. Results

4.1. Annual Precipitation

[13] The mean annual precipitation climatology of Spain for present climate as calculated from Spain02 is provided in Figure 2 to be used as a reference. Figure 2 also illustrates 10 rainfall affinity regions obtained using a multistep regionalization methodology [*Argüeso et al.*, 2011, 2012] that was applied to daily values of Spain02.

[14] The changes projected by the regional model in the annual precipitation means are shown in Figure 3. All WRF simulations project a substantial decrease in annual precipitation by the end of the century (2070–2099) with respect to present conditions (1970–1999) over almost the entire Spain, with a few exceptions in the east coast.

[15] In average over Spain, the changes range from −18% (WEB1) to −42% (WCA2), which are in accordance with previous results [*Gao and Giorgi*, 2008; *van der Linden and Mitchell*, 2009]. Simulations driven by both GCMs respond to GHGs atmospheric concentration in the same direction and precipitation decreases tend to be larger under higher GHGs emissions scenarios. However, there are regions, such as the northern Atlantic coast, where changes do not seem to present a strong dependency upon the boundary conditions and the projections are similar even under different emissions scenarios.

[16] Broadly speaking, the precipitation changes show a gradient from largest in the southern half of Spain to the most moderate toward the north, which was already observed in the GCMs projections [*Intergovernmental Panel on Climate Change* (*IPCC*), 2007]. Nonetheless, the high spatial resolution makes it possible to identify regions within Spain that might be particularly exposed to future changes. To be specific, the mountainous areas are likely to be affected by severe changes, especially in the southeast, where precipitation is expected to decrease approximately between −30% and −65%. The southeast, and more particularly the mountains located there, is systematically projected (all 6 simulations) to be the most affected region in terms of precipitation reduction. If previous studies at lower spatial resolution [*Gao et al.*, 2006; *Sánchez et al.*, 2004; *Buonomo et al.*, 2007; *Kjellström et al.*, 2010] are considered, the results presented here might be regarded as an evidence of the improved spatial detail that these high-resolution simulations provide, as well as a good indicator of the robustness of current RCMs projections. However, it must also be mentioned that despite the fact that ENSEMBLES runs [*van der Linden and Mitchell*, 2009] project similar changes in this region, they are not conclusive with respect to this matter. Precipitation in the southeastern mountains feeds one of the most productive agricultural regions in Europe and these changes could undoubtedly undermine future current production due to future water shortage. In the rest of the mountainous areas, the precipitation decrease is also noteworthy, above −30% in most of the runs.

[17] Despite the fact that there are a few areas along the Mediterranean coast where some simulations suggest slight increases in total annual precipitation, it must also be noted that they barely exceed 10% and are statistically non-significant according to a two-sided Student's t-test at the 95% confidence level (flagged with black dots in Figure 3). Actually, under the non-intervention A2 scenario, the entire Spain would be subjected to negative changes and the areas with severe reductions would not be restricted to the south, but would cover most of the Peninsula. Indeed, half of Spain might experience decreases over the −30% by the end of the century and even larger if the CCSM-driven simulation is considered.

4.2. Seasonal Precipitation

[18] Iberian precipitation is strongly seasonal (Figure 4) and the mechanisms producing rainfall are not the same through the year, and thus the projected changes might differ too. Accordingly, the seasonal changes are analyzed here to elucidate how seasonal precipitation might evolve under climate change conditions. Figure 5 illustrates precipitation changes for winter (DJF) and summer (JJA) as projected by WRF simulations driven by ECHAM5 and CCSM respectively. For brevity, spring and autumn maps are omitted, but results are summarized in Table 2, where the spatial average of the changes over Spain for all simulations is displayed. Additionally, Table 3 describes the changes spatially averaged over the 10 precipitation regions (shown in Figure 2b) for simulations under A1B conditions to provide an overview of the spatial distribution of the changes.

[19] In line with previous results for the Mediterranean area [*Giorgi and Lionello*, 2008; *IPCC*, 2007], the largest reduction of precipitation is projected to occur during the summer, when rainfall might decrease between −32% (WEB1and WEA1B) and −72% (WCA2), in average over Spain. All simulations consistently locate large precipitation decreases along the eastern coast, but notable changes are projected by some simulations in other regions as well. For instance, the south and southwestern might be exposed to decreases above −60% according to CCSM-driven simulations. In the case of WCA2, most of Spain is likely to experience decreases in summer precipitation above −70%. On the other hand, ECHAM5-driven simulation suggest more moderate changes that would only exceed −60% under the A2 scenario. Most of the changes are largely significant except for areas such as the south of Spain, where the information downscaled from ECHAM5 (WEB1 and WEA1B) did not produce statistically significant changes.

[20] Summer is the dry season in the IP, precipitation amounts are usually very low and the number of events tend to be very few even in the present, especially in the southern half. As a consequence, small changes in the number of rain

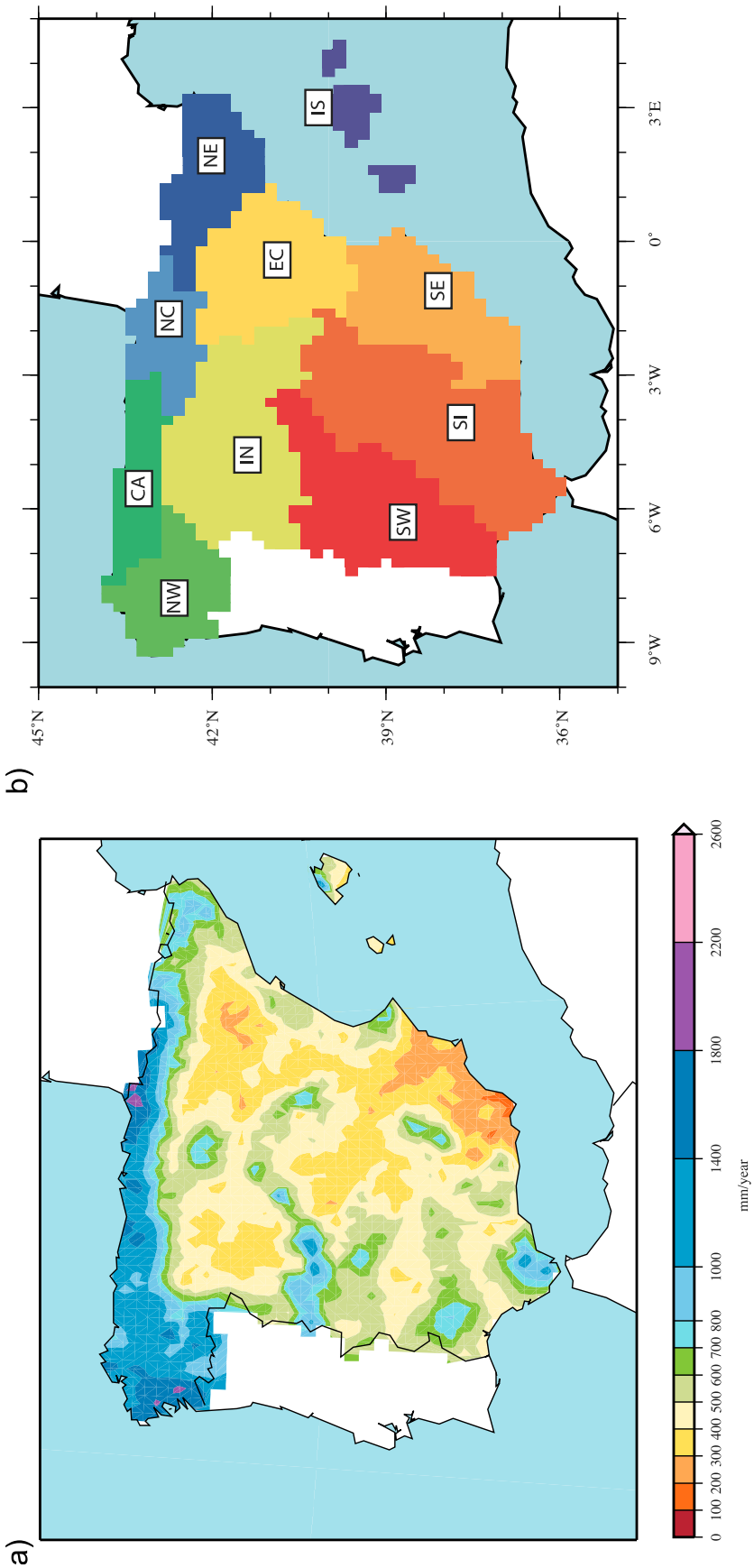

Figure 2. (a) Annual mean precipitation climatology over Spain using Spain02 dataset. (b) Ten precipitation affinity regions obtained for Spain using a multistep regionalization methodology (S-Mode PCA, agglomerative clustering and non-hierarchical clustering) and Spain02: Northwest (NW), Cantabrian Range (CA), North central (NC), Northeast (NE), Interior (IN), East central (EC), Islands (IS), Southwest (SW), South interior (SI) and Southeast (SE).

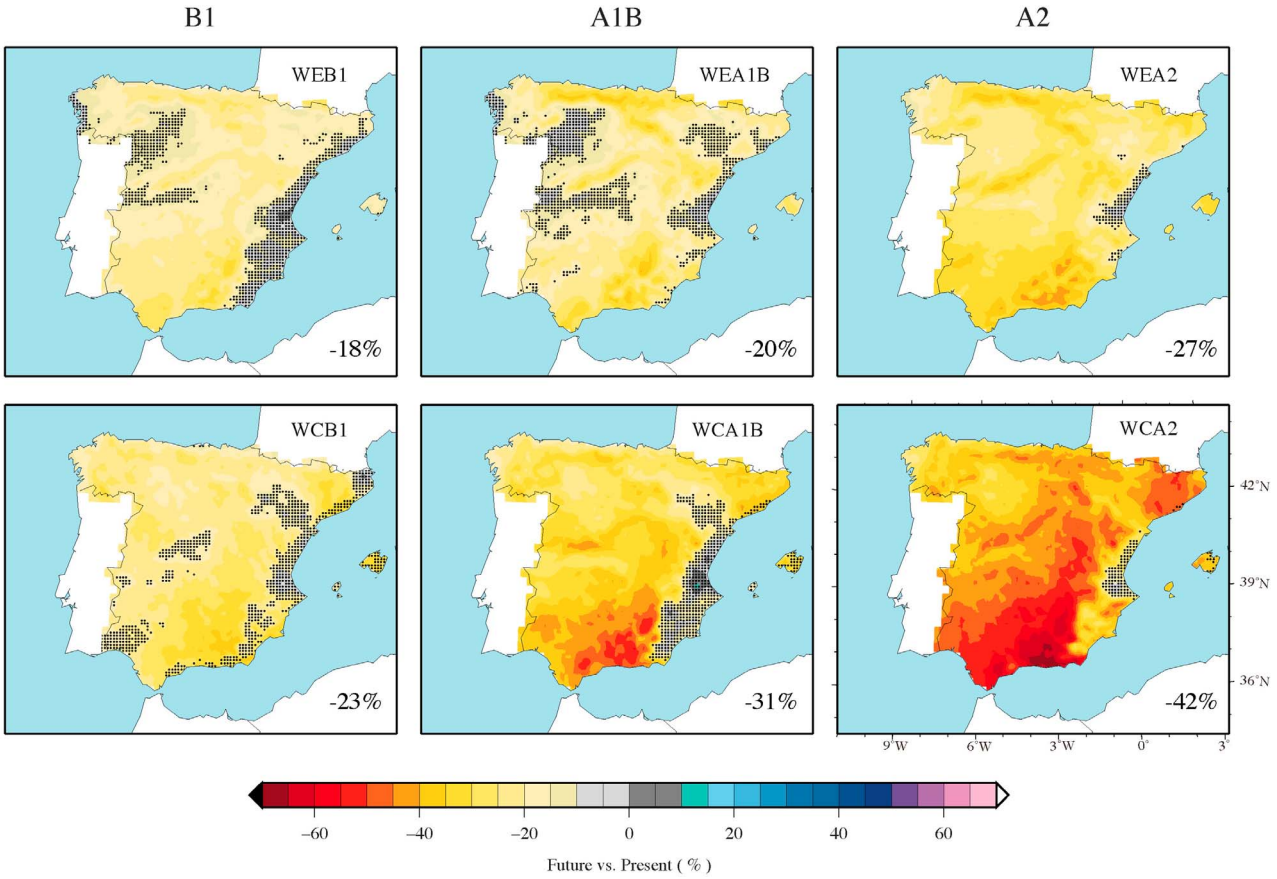

Figure 3. Projected changes in the annual mean precipitation (2070–2099 versus 1970–1999) for the different WRF simulations. Areas with black dots indicate that changes are not significant using a two-sided Student's t-test at the 95% confidence level. The spatially averaged changes over Spain are shown in the bottom right corner of each panel.

days could lead to large relative changes in summer rainfall, which might explain the inconsistencies between the projections. Although the contribution of summer precipitation to annual total amounts is usually unimportant, summer changes should not be disregarded because considerable decreases during this season might be critical to natural environment, particularly in terms of fire risk and hydrological stress. But also to humans due to urban atmosphere pollution events.

[21] Unlike summer, winter precipitation might be expected to increase over certain areas in Spain, even though these changes are generally small. According to WRF simulations, still a large fraction of Spain will be subjected to decreases during the winter. Indeed, the northern coast is systematically projected to suffer from decreases in winter precipitation. These projections are remarkably consistent, since they are statistically significant in all simulations and show very little dependence upon the boundary conditions. Although not being fully comparable because of the spatial resolution disparity and the complex topography of the area, these results compare well with ENSEMBLES simulations [*van der Linden and Mitchell*, 2009], which project a particularly pronounced decrease over the Cantabrian Range during the winter. The positive changes are considerably marked over parts of the Peninsula, such as the Mediterranean coast and the Northern Central Plateau, although in general they are not statistically significant. On average over Spain, winter changes are likely to range between −2% (WEA1B) and −23% (WCA2).

[22] Spring and autumn changes have also been calculated and are negative over the entire Spain (Tables 2 and 3). They actually behave as transition seasons between the changes projected for winter and summer. Spring decreases are between −24% (WEB1) and −58% (WCA2), and are significant over most of Spain. As for the autumn, the changes fall between −23% (WEB1 and WEA1B) and −50% (WCA2), even though under the B1 and to a lesser extent, the A1B scenarios, they are partly significant and partly not. The spatial distribution of these changes is rather homogeneous, but tend to be larger in the southern part of the IP and particularly noteworthy over the mountainous areas, reaching down to −75% in the A2 scenario. In the case of CCSM-driven, the largest spring changes are rather located along the east coast. Actually, the spatial pattern of annual mean changes is very similar to those obtained for spring and autumn due to their contribution to total annual amounts.

4.3. Daily Precipitation

[23] The analysis of daily precipitation makes it possible to determine the nature of the changes, discern which kind of events might change substantially and outline the precipitation

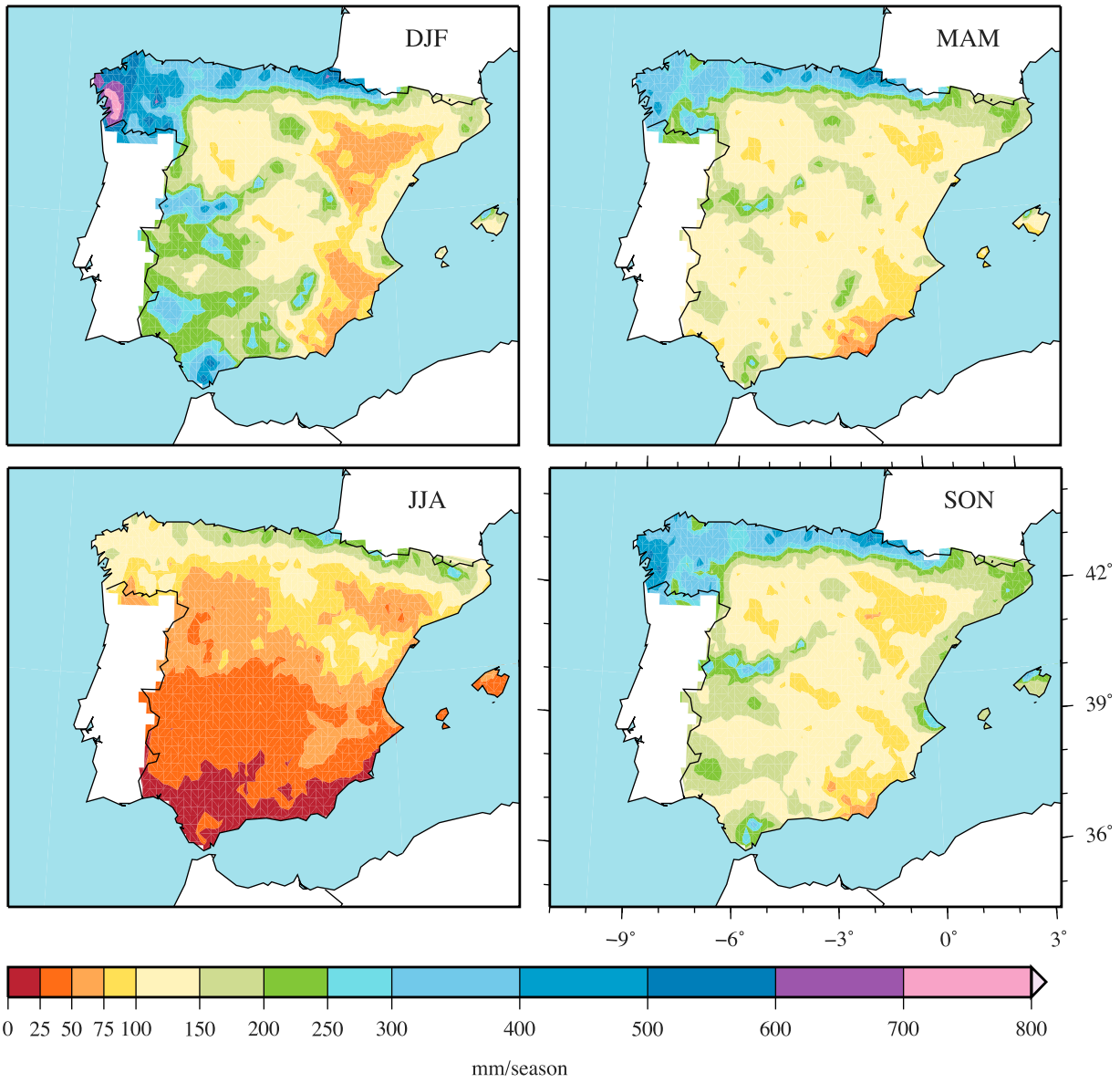

Figure 4. Seasonal mean precipitation climatology over Spain using Spain02 dataset.

regimes in the future. To explore changes in the frequency and intensity of daily events, the 10 rainfall affinity regions (Figure 2b) were used to provide a more comprehensive examination. For each of the regions, the quantile-quantile (q-q) plots (future versus present) and the contribution to total precipitation by different-intensity events were analyzed considering only wet days (≥0.1 mm/day). The latter is represented by a sort of probability density function (PDF), the pseudo-PDF, which is a histogram that illustrates the product of the number of events by the mean intensity in each bin. This overcomes the problem of masking light (≤5 mm/day) or heavy (≥50 mm/day) precipitation changes by the traditional PDF depending on the scale (log or linear). Instead, the pseudo-PDF allows for easy and direct interpretation of the importance of the changes with respect to total precipitation. Figure 6 shows the projected changes in terms of percentiles and pseudo-PDF for two representative regions in Spain: Northwest (NW) and Southeast (SE). These two regions are selected because the rest of the regions show a similar response to climate change to either NW or SE in terms of their pseudo-PDF changes.

[24] The changes in the pseudo-PDF reveal that light-to-moderate (≤30 mm/day) events are likely to considerably decrease (down to approximately −50% in the SW for WCA2, not shown), whereas the number of heavy rainfall events are projected to remain constant or slightly increase in the future for all regions. These results are in accordance with previous analysis of the changes in the PDF using another RCM within the frame of PRUDENCE project [*Boberg et al.*, 2009], which evinced a similar pattern of the changes for the entire Spain. However, it contrasts with results from *Boberg et al.* [2010], which examined projections by a RCM from ENSEMBLES project that indicate almost no changes over the IP. It must also be stated that the IP was the region with higher discrepancies for low precipitation intensities (and substantial underestimation of extreme events) between the RCMs in ENSEMBLES

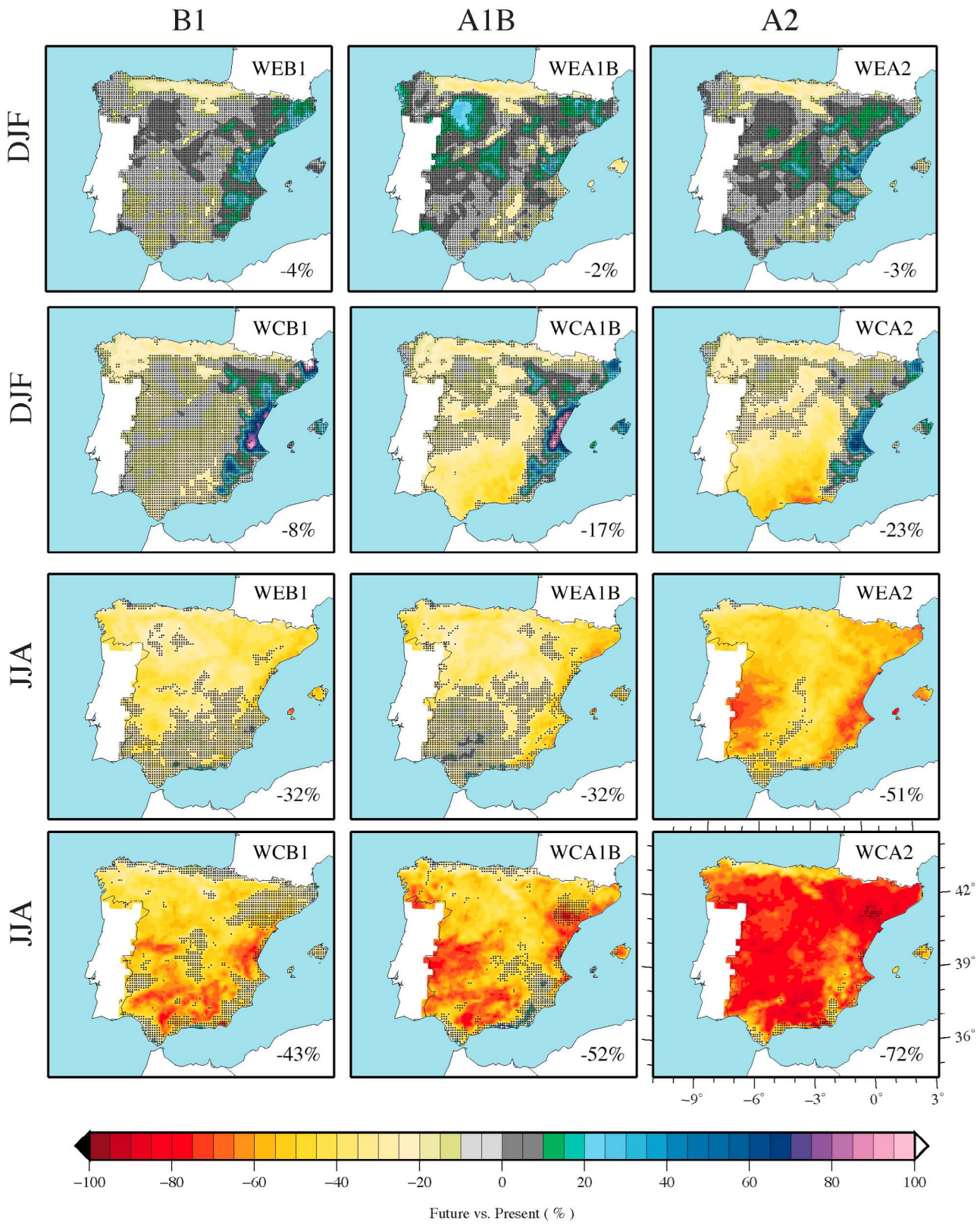

Figure 5. WRF projected changes for (top) DJF and (bottom) JJA precipitation (2070–2099 versus 1970–1999). Results for the B1, A1B and A2 scenarios are displayed in columns. Areas with black dots indicate that changes are not significant using a two-sided Student's t-test at the 95% confidence level. The spatially averaged changes over Spain are shown in the bottom right corner of each panel.

Table 2. Seasonal Changes (%) Spatially Averaged Over Spain for Each of the Simulations

	Simulation	DJF	MAM	JJA	SON
B1	WEB1	−4	−24	−32	−23
	WCB1	−8	−37	−43	−25
A1B	WEA1B	−2	−34	−32	−23
	WCA1B	−17	−47	−52	−33
A2	WEA2	−3	−41	−51	−38
	WCA2	−23	−58	−72	−50

and the observations. The changes of the pseudo-PDF projected here suggest that the annual decreases are a result of less events within the range 1–30 mm/day and the precipitation extreme events are not expected to significantly change in number, although their relative probability would increase. As a consequence, the Spanish precipitation is projected to be concentrated in fewer rain days and the probability density function would be displaced toward heavier precipitation. *Boberg et al.* [2009, 2010] have also analyzed changes in the PDF over this region and, despite the fact that they explore the PDF of the entire IP at once and thus are difficult to compare with our results, they both obtained a similar shape of the projected changes, suggesting a displacement of the PDF toward higher values. According to our simulations, these changes tend to be more intense as higher GHGs emissions are considered (from B1 to A2 scenarios).

[25] It is worth mentioning that despite the different pseudo-PDF produced by CCSM- and ECHAM5-driven simulations, the projected changes are fairly similar in relative terms, with respect to the corresponding present climate runs. They both project almost no changes in events above 50 mm/day and decreases in the number of events below 30 mm/day, which stresses the consistency of the displacement toward heavier rainfall in the future. Nonetheless, there is a noticeable difference in the projected contribution of very extreme events (≥80 mm) to annual precipitation by the two groups of simulations. For instance, those runs forced by ECHAM5 suggest an increase in the contribution of these evens in some regions, whereas those constrained by CCSM systematically show a decreasing tendency.

[26] Concerning the upper-percentiles (90th and 95th), ECHAM5-driven simulation project slight increases in all regions (only changes for NW and SE regions are shown in Figure 6), except in two of them located in the northern coast (CA and NC); whereas CCSM-driven simulations do not show a clear tendency and both minor increases and decreases in the intensity of very extreme events might be expected. To be subjected to the largest changes are those events above the 95th, which might change up to 10 mm over particular regions, whereas events below the 95th might only suffer from minor changes that barely exceed 5 mm. As for the different scenarios, there does not seem to be a direct relationship between the changes in the percentiles and the emission scenarios, as evidenced by the fact that the changes are not consistently larger for any of them. The changes in the magnitude of the upper percentiles are not overall substantial and the relevance of the changes in extremes might be rather related to the persistence of extreme conditions or the intensity of several-day events.

4.4. Extreme Events

[27] An excerpt of the extreme indices proposed by Expert Team on Climate Change Detection and Indices (ETCCDI) (http://cccma.seos.uvic.ca/ETCCDI/indices.shtml) was selected to further characterize changes in extreme precipitation. Specifically, 6 indices were singled out and calculated on a yearly basis: maximum 5-consecutive-day precipitation (Rx5day), percentage of total precipitation above the 95th daily percentile (R95T), number of days with precipitation above 10 mm and 20 mm (R10 and R20) and annual mean maximum number of consecutive wet and dry periods (CWD* and CDD*). The latter indices are modified versions of the original CWD and CDD indices, which are defined as the maximum number of consecutive dry (wet) days over the entire period, using a 0.1 mm/day threshold to define a dry/wet day. Since the original definition is very sensitive to small changes or deviations, these indices are calculated here for each of the years and their mean climatological values are employed as the new indices in order to gain robustness. These new versions of CWD and CDD are now referred as CWD* and CDD*. The significance of these changes was tested using a two-tailed Kolmogorov-Smirnov test following *Avila et al.* [2012], which let us reject the hypothesis that both data samples are extracted from the same distribution.

[28] Figure 7a illustrates the projected changes for the Rx5day index. The Rx5day changes are highly dependent on the region considered and the GCMs employed to drive WRF, although there not seem to be a clear dependency upon the emission scenario. Both positive and negative changes for this index were projected by all simulations and no evident tendency was suggested in general. Nonetheless, there are areas within Spain that were consistently projected to suffer from substantial increases in the 5-day maximum precipitation, such as the eastern coast. Indeed, all simulations project changes that might reach up to 150% in the central part of the Mediterranean coast (although they are generally non-significant), excluding WCB1 that projects smaller changes. Present-climate precipitation in this area is already characterized by heavy rainfall, particularly in the late summer and early autumn, which could intensify in the future as suggested by WRF simulations.

[29] Overall, the ECHAM5-driven runs indicate a decrease in the Southern Central Plateau and some parts of the Iberian System. Decreases of the Rx5day index are also projected in certain areas across Spain (southwest, southeast coast and the Cantabrian Range), but they often alternate with areas where the index is projected to increase notably. In fact, the spatial distribution is quite different among these

Table 3. Seasonal Changes (%) for Each of the 10 Regions and Under the A1B Scenario

	Simulation	SW	SI	SE	EC	IN	NW	CA	NC	NE	IS
DJF	WEA1B	3	−4	−6	3	5	1	−24	−18	5	−28
	WCA1B	−23	−34	7	12	−16	−16	−24	−15	−1	35
MAM	WEA1B	−36	−39	−32	−35	−34	−30	−34	−31	−27	−27
	WCA1B	−49	−50	−40	−52	−47	−39	−34	−41	−55	−69
JJA	WEA1B	−26	−20	−40	−37	−33	−35	−35	−33	−48	−37
	WCA1B	−65	−51	−33	−58	−48	−52	−34	−38	−50	−41
SON	WEA1B	−23	−31	−19	−15	−17	−22	−29	−28	−20	−12
	WCA1B	−44	−49	−25	−14	−32	−27	−20	−15	−34	−32

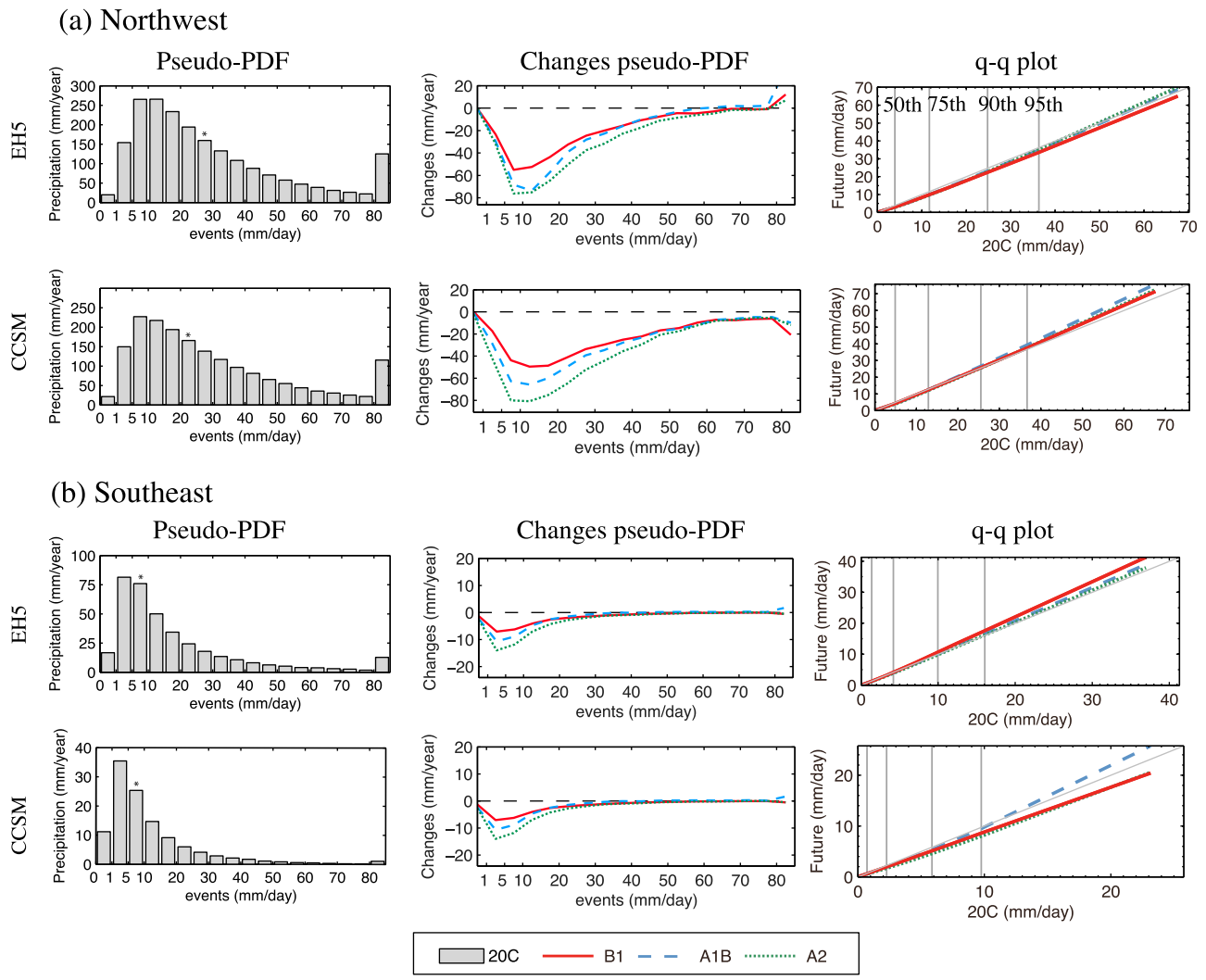

Figure 6. Projected changes in the intensity distribution of daily events (2070–2099 versus 1970–1999). (left) Present-climate contribution to total precipitation by different-intensity events (pseudo-PDF). The star indicates the location of the 90th percentile. (middle) The changes of the pseudo-PDF. (right) The changes in the percentiles (q-q plots). The vertical grey lines in the q-q plots represent the 50th, 75th, 90th and 95th present-climate percentiles. In rows are organized the simulations using ECHAM5 and CCSM. A sample of two regions was selected: (a) Northwest and (b) Southeast.

simulations and only broad characteristics are common to all three, such as the increase in the Northern Central Plateau (up to 60%). By contrast, the spatial patterns of Rx5day projections are somehow more consistent among CCSM-driven simulations. Indeed, certain areas are systematically projected to suffer from decreases in the Rx5dayindex, such as the Cantabrian coast, the south of Spain, where the index might be less severe than in the present. The central Mediterranean coast and the area limited by the Central System and Sierra Morena might be affected by larger 5-day maximum precipitation in the future, according to runs constrained by CCSM.

[30] The effects of less precipitation and more concentrated in extreme events are observed as a whole in the R95T index (Figure 7b), which illustrates the displacement of the probability distribution function toward higher precipitation daily values. Changes in the total amount of precipitation explained by events above the 95th percentile manifest the relative probability rise of extreme events to occur. Large areas of the IP are projected to suffer from increases in the R95T index. The changes are expressed in terms of differences between future and present percentages, and thus in percentage units. Most changes fall within the range between 0 and 2 percentage units, but there are also regions where the increments in R95T reach up to about 4 percentage units. These changes might be particularly severe near the Mediterranean coast, where R95T could increase in up to 8 percentage units (WCA1B and WCA2), which would lead to R95T values over 35%, bearing in mind the present-climate values. Other noticeable changes suggested by most of the simulations are observed in the Baetic System, the northwest and the Northern Central Plateau, although the spatial distributions within these areas are not common to all runs. It is worth noting that there are also regions where R95T is projected to decreases, such as the low Ebro Valley (down to −9 percentage units), although all experiments provide

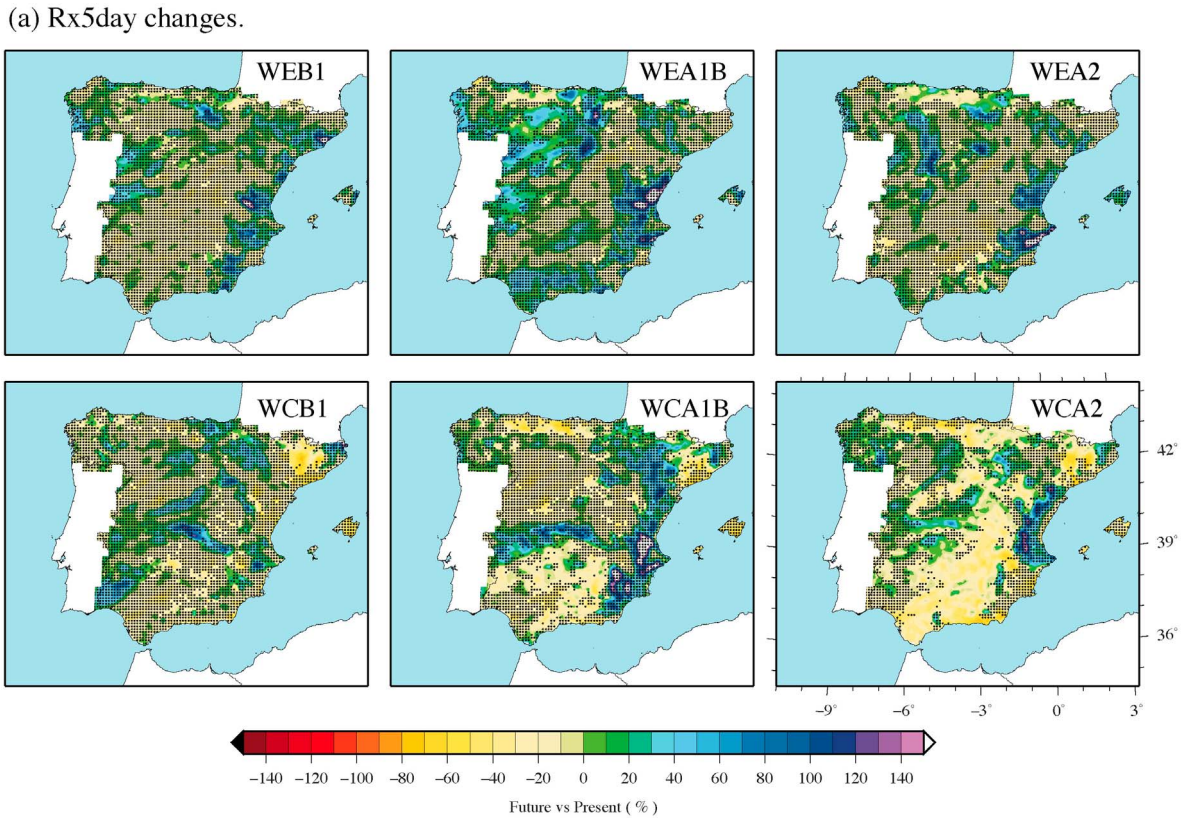

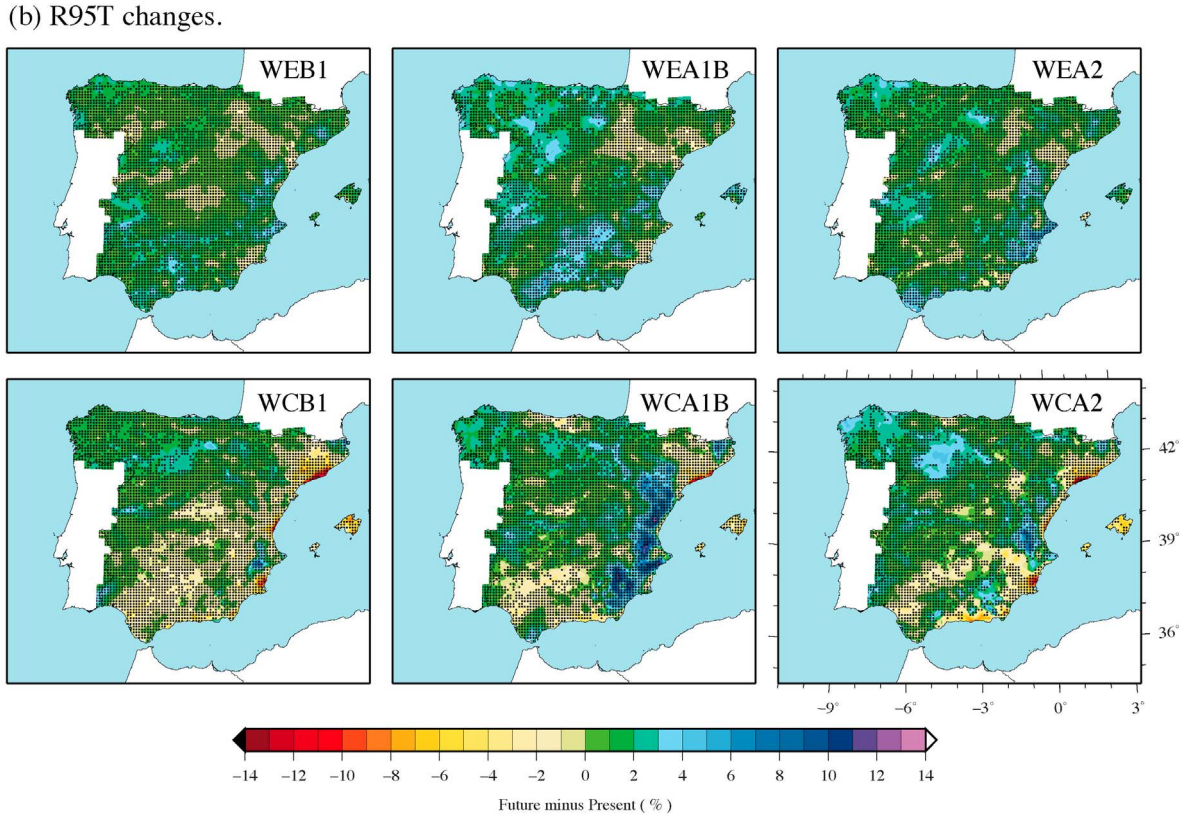

Figure 7. Projected changes in (a) the Rx5day index (2070–2099 versus 1970–1999) and (b) the R95T index (2070–2099 minus 1970–1999) for the different WRF simulations. Changes in Rx5day are expressed in relative terms, whereas for R95T are expressed as differences between future and present percentages. Areas with black dots indicate that the hypothesis of equal distribution of the data cannot be rejected using a two-sided Kolmogorov-Smirnov test at the 95% confidence level.

evidences of an overall tendency toward larger percentages of precipitation accumulated in the furthest part of the distribution.

[31] The moderate events are explored through the R10 and R20 indices. Figure 8a shows the projected changes for the R10, which are in accordance with the results for the pseudo-PDF and show spatial patterns very similar to those for the annual mean changes. This supports the idea that a large portion of the annual precipitation decrease is due to less light-to-moderate events. Although some simulations project slight increases limited to small regions, such as the interior and the Mediterranean coast, R10 is likely to decrease between −10% and −40% almost all over Spain according to all WRF simulations. Over the Baetic System, the Southern Central Plateau and the northernmost Mediterranean coast, changes might be particularly remarkable, since the decreases in the R10 index could arrive at −70% (WCA2).

[32] Regarding more intense events, the R20 index projections (Figure 8b) show both substantial positive and negative changes might be expected across Spain. The largest increases are generally located in areas of Spain that are especially dry: Northern Central Plateau, Ebro Valley and eastern coast. They are particularly large in the former, where R20 could increase over 30%. As for the negative changes in R20, they are mostly observed in the Cantabrian Range and the south (down to −70% in the CCSM-driven runs). Some of these areas are systematically projected to respond similarly, which emphasize the consistency of WRF projections in terms of R20.

[33] Besides the intensity of events, it is also interesting to evaluate changes in the persistence of dry and wet periods, which might be of paramount importance to the environment and the water availability, particularly in areas where precipitation is not very frequent. The persistence of these periods is characterized by CDD* and CWD*, respectively. Figure 9 illustrates the projected changes for both indices and overall, the wet periods are projected to be shorter in the future, whereas the dry spells are likely to be longer. There is also a dependency upon the emission scenario and this tendency becomes more prominent for higher GHGs concentrations. *Sánchez et al.* [2011] also studied the evolution of dry spells under climate change conditions and obtained similar results, although the indices by them employed were different.

[34] The changes in CWD* (Figure 9a) indicate that the length of continuous wet periods is likely to decrease over nearly the entire Spain, with very few exceptions in areas along the east coast. The spatial distribution of these changes is fairly similar among simulations and the most substantial changes are located along the Cantabrian coast, where CWD* might drop by 50%. In addition, the Baetic System and Sierra Morena are also projected to undergo important decreases. Conversely, the duration of the wet spells is likely to be larger in the Mediterranean coast and, to a lesser extent, in the Ebro valley, according to simulations under the B1 scenario. The CWD* could also be slightly higher in some areas in the interior and the northwest, but the extension of these areas is certainly limited.

[35] As for the consecutive dry days (Figure 9b), CDD* suggests that the length of the dry periods might be expected to increase all over the region, especially in the northern half of Spain. However, near the northern coast, there is a narrow strip delimited by the mountains where CDD* is projected to increase much less or even slightly decrease (very confined spots). The largest increases are observed in the surroundings of the Galician Massif, to the south of the Cantabrian Range and in the Pyrenees. Even under the scenarios for which the changes are more moderate, the CDD* might increase by up to 60% in these areas, whereas it would change in about 20% for the rest of Spain. The areas where these changes are significant are larger as we move from B1 to A2 scenarios, covering most of Spain under the A2.

5. Conclusions

[36] The high-resolution climate simulations provide several evidences of a substantially drier climate over nearly the entire Spain by the end of this century. The mountainous areas, and more specifically the southern ones, might be particularly affected by these precipitation decreases. Very confined areas could be subjected to minor decreases or even slight increases, although these changes are statistically nonsignificant. A clear dependency of these results upon the GHGs atmospheric concentration was also observed, as the changes tend to be more severe as we move from B1 to A2 scenarios.

[37] Except for the winter, all seasons are projected to experience precipitation decreases nearly over the entire Spain. On spatial average, Spain will be subjected to precipitation decreases during all seasons and according to all WRF simulations. They are especially marked during the summer. The Iberian summer is generally dry and a further reduction in precipitation could enhance summer warming due to surface fluxes redistribution. The region is already subjected to periodical droughts with important effect on human activity that could intensify in the future. Actually, the length of consecutive dry (wet) conditions is projected to increase (decrease) almost all over Spain. As a consequence, the region might be exposed to longer droughts that could compromise water availability.

[38] These precipitation decreases are mainly caused by reduction in the light-to-moderate rainfall events. The frequency of extreme events is not likely to change substantially, although their relative probability could be larger in the future due to decreases in the light-to-moderate precipitation. Therefore, Spain might be characterized in the future by less precipitation but more concentrated in heavy rainfall events.

[39] Overall, no consistent signal was projected regarding very extreme rainfall intensity (≥80 mm/day) because the projections are highly dependent on the boundary conditions, apart from the central Mediterranean coast and the northwest, where heavy rainfall might be expected to strengthen. In fact, in these areas, the percentage of total precipitation explained by upper-percentile events is systematically projected to increase. The Mediterranean coast is already exposed to recurrent and very local downpours that have an important socio-economic impact on the region, and hence the risk could increase in the future.

[40] This study provides a detailed picture of precipitation changes over Spain at different timescales, which constitutes a valuable reference to following impact assessments. Nonetheless, the results foster further investigation on the

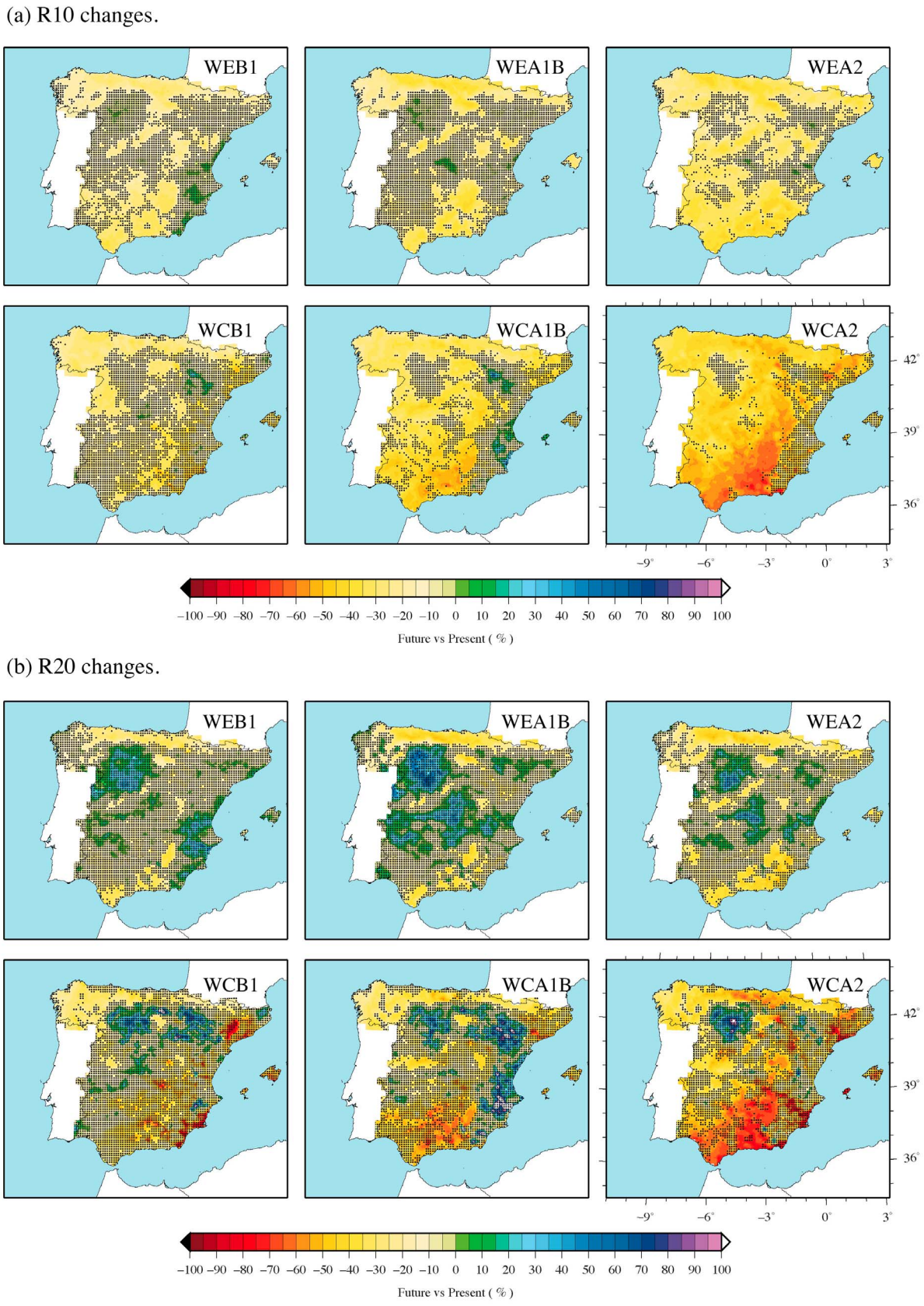

Figure 8. Projected changes in (a) the R10 and (b) R20 indices (2070–2099 versus 1970–1999) for the different WRF simulations. Areas with black dots indicate that the hypothesis of equal distribution of the data cannot be rejected using a two-sided Kolmogorov-Smirnov test at the 95% confidence level.

(a) CWD* changes.

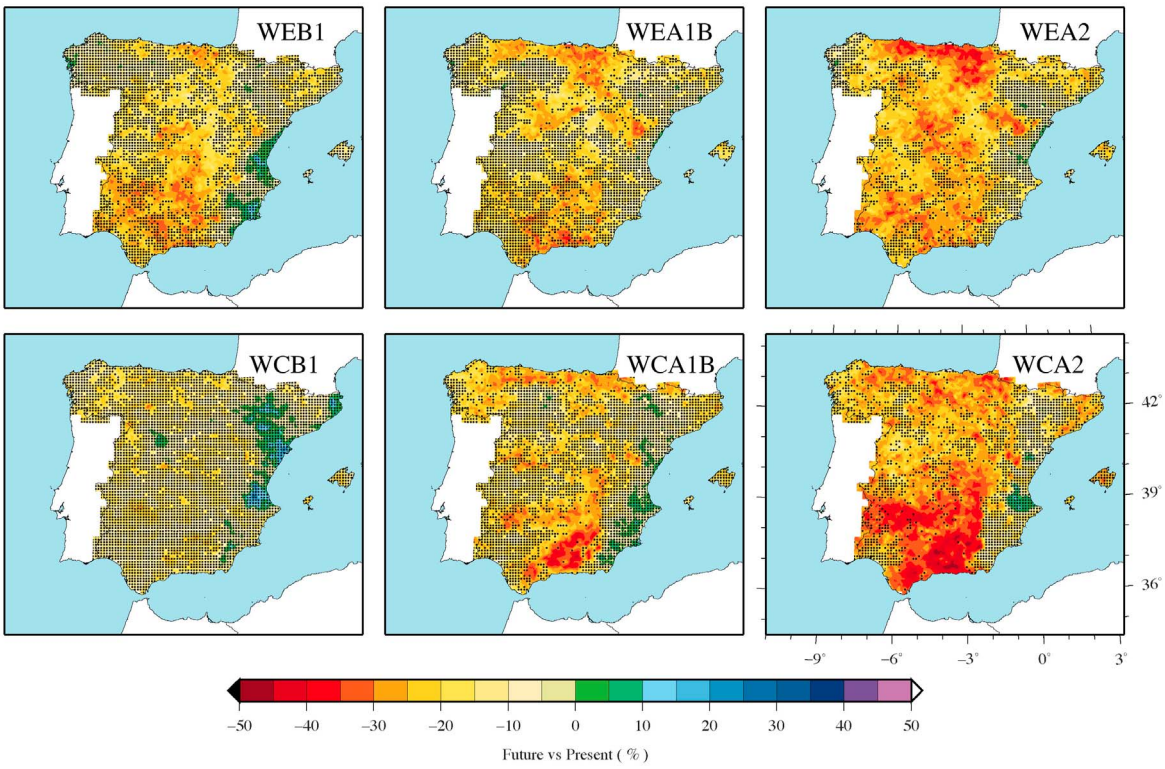

(b) CDD* changes.

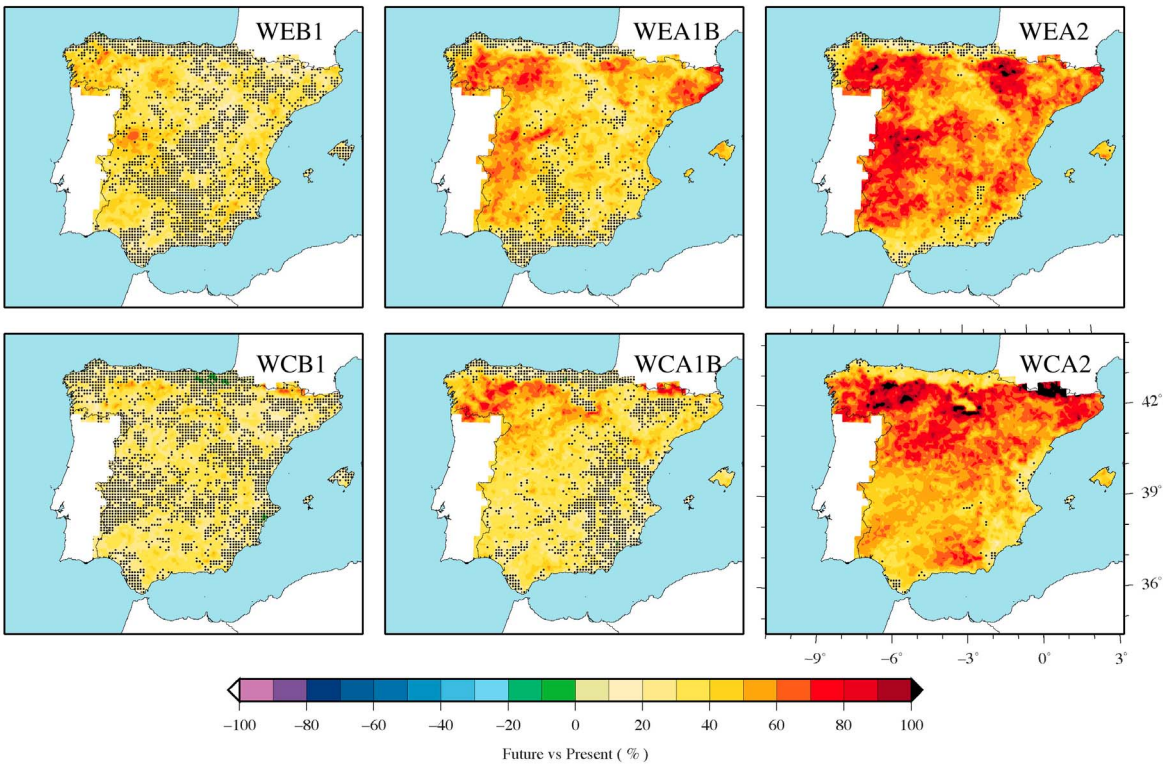

Figure 9. WRF projected changes in the (a) CWD* and (b) CDD* indices (2070–2099 versus 1970–1999). The columns show the B1, A1B and A2 scenarios. The rows show the GCMs employed to drive WRF. Areas with black dots indicate that the hypothesis of equal distribution of the data cannot be rejected using a two-sided Kolmogorov-Smirnov test at the 95% confidence level.

effect of global warming on extreme precipitation and persistent dry conditions in order to reduce the inconsistencies among the different simulations.

[41] **Acknowledgments.** The Spanish Ministry of Science and Innovation, with the additional support from the European Community funds (FEDER), project CGL2010–21188/CLI, and the Regional Government of Andalusia, project P06-RNM–01622, have financed this study. The "Centro de Servicios de Informática y Redes de Comunicaciones" (CSIRC), Universidad de Granada, has provided the computing time.

References

Argüeso, D., J. M. Hidalgo-Muñoz, S. R. Gámiz-Fortis, M. J. Esteban-Parra, J. Dudhia, and Y. Castro-Díez (2011), Evaluation of WRF parameterizations for climate studies over southern Spain using a multi-step regionalization, *J. Clim.*, *24*(21), 5633–5651, doi:10.1175/JCLI-D-11-00073.1.

Argüeso, D., J. Hidalgo-Muñoz, S. Gámiz-Fortis, M. Esteban-Parra, and Y. Castro-Díez (2012), Evaluation of WRF mean and extreme precipitation over Spain: Present climate (1970–1999), *J. Clim.*, in press.

Avila, F. B., A. J. Pitman, M. G. Donat, L. V. Alexander, and G. Abramowitz (2012), Climate model simulated changes in temperature extremes due to land cover change, *J. Geophys. Res.*, *117*, D04108, doi:10.1029/2011JD016382.

Bell, J., L. Sloan, and M. Snyder (2004), Regional changes in extreme climatic events: A future climate scenario, *J. Clim.*, *17*(1), 81–87.

Beniston, M., et al. (2007), Future extreme events in European climate: An exploration of regional climate model projections, *Clim. Change*, *81*(S1), 71–95, doi:10.1007/s10584-006-9226-z.

Betts, A., and M. Miller (1986), A new convective adjustment scheme. Part II: Single column tests using GATE wave, BOMEX, ATEX and arctic air-mass data sets, *Q. J. R. Meteorol. Soc.*, *112*(473), 693–709.

Boberg, F., P. Berg, P. Thejll, and W. Gutowski (2009), Improved confidence in climate change projections of precipitation evaluated using daily statistics from the PRUDENCE ensemble, *Clim. Dyn.*, *32*, 1097–1106, doi:10.1007/s00382-008-0446-y.

Boberg, F., P. Berg, P. Thejll, W. J. Gutowski, and J. H. Christensen (2010), Improved confidence in climate change projections of precipitation further evaluated using daily statistics from ENSEMBLES models, *Clim. Dyn.*, *35*, 1509–1520.

Bukovsky, M. S., and D. J. Karoly (2011), A regional modeling study of climate change impacts on warm-season precipitation in the central United States, *J. Clim.*, *24*(7), 1985–2002, doi:10.1175/2010JCLI3447.1.

Buonomo, E., R. G. Jones, C. Huntingford, and J. Hannaford (2007), On the robustness of changes in extreme precipitation over Europe from two high resolution climate change simulations, *Q. J. R. Meteorol. Soc.*, *133*(622), 65–81, doi:10.1002/qj.13.

Caldwell, P., H.-N. S. Chin, D. C. Bader, and G. Bala (2009), Evaluation of a WRF dynamical downscaling simulation over California, *Clim. Change*, *95*(3–4), 499–521, doi:10.1007/s10584-009-9583-5.

Castro, M., C. Gallardo, K. Jylha, and H. Tuomenvirta (2007), The use of a climate-type classification for assessing climate change effects in Europe from an ensemble of nine regional climate models, *Clim. Change*, *81*(S1), 329–341, doi:10.1007/s10584-006-9224-1.

Chen, F., and J. Dudhia (2001), Coupling an advanced land surface-hydrology model with the Penn State-NCAR MM5 Modeling System part I: Model implementation and sensitivity, *Mon. Weather Rev.*, *129*, 569–585.

Christensen, J., et al. (2007a), Regional climate projections, in *Climate Change 2007: The Physical Science Basis. Contribution of Working Group I to the Fourth Assessment Report of the Intergovernmental Panel on Climate Change*, edited by S. Solomon et al., pp. 847–940, Cambridge Univ. Press, Cambridge, U. K.

Christensen, J. H., T. R. Carter, M. Rummukainen, and G. Amanatidis (2007b), A summary of the PRUDENCE model projections of changes in European climate by the end of this century, *Clim. Change*, *81*, 1–6.

Collins, W. D., et al. (2004), Description of the NCAR Community Atmosphere Model (CAM 3.0), *NCAR Tech. Note, NCAR/TN-464 + STR*, pp. 1–226, Natl. Cent. for Atmos. Res., Boulder, Colo.

Collins, W. D., et al. (2006), The Community Climate System Model version 3 (CCSM3), *J. Clim.*, *19*(11), 2122–2143.

Denis, B., R. Laprise, D. Caya, and J. Côte (2002), Downscaling ability of one-way nested regional climate models: The Big-Brother Experiment, *Clim. Dyn.*, *18*(8), 627–646, doi:10.1007/s00382-001-0201-0.

Esteban-Parra, M. J., F. S. Rodrigo, and Y. Castro-Díez (1998), Spatial and temporal patterns of precipitation in Spain for the period 1880–1992, *Int. J. Climatol.*, *18*(14), 1557–1574.

Evans, J. P., and M. F. McCabe (2010), Regional climate simulation over Australia's Murray-Darling basin: A multitemporal assessment, *J. Geophys. Res.*, *115*, D14114, doi:10.1029/2010JD013816.

Fernández, J., J. P. Montávez, J. Sáenz, J. González-Rouco, and E. Zorita (2007), Sensitivity of the MM5 mesoscale model to physical parameterizations for regional climate studies: Annual cycle, *J. Geophys. Res.*, *112*, D04101, doi:10.1029/2005JD006649.

Fita, L., and J. Fernández (2010), CLWRF: WRF modifications for regional climate simulation under future scenarios, paper presented at 11th WRF Users' Workshop, Natl. Cent. for Atmos. Res., Boulder, Colo.

Frei, C., J. H. Christensen, M. Déqué, D. Jacob, R. G. Jones, and P. L. Vidale (2003), Daily precipitation statistics in regional climate models: Evaluation and intercomparison for the European Alps, *J. Geophys. Res.*, *108*(D3), 4124, doi:10.1029/2002JD002287.

Gao, X., and F. Giorgi (2008), Increased aridity in the Mediterranean region under greenhouse gas forcing estimated from high resolution simulations with a regional climate model, *Global Planet. Change*, *62*(3–4), 195–209, doi:10.1016/j.gloplacha.2008.02.002.

Gao, X., J. Pal, and F. Giorgi (2006), Projected changes in mean and extreme precipitation over the Mediterranean region from a high resolution double nested RCM simulation, *Geophys. Res. Lett.*, *33*, L03706, doi:10.1029/2005GL024954.

Ge, J., J. Qi, B. Lofgren, N. Moore, and N. Torbick (2007), Impacts of land use/cover classification accuracy on regional climate simulations, *J. Geophys. Res.*, *112*, D05107, doi:10.1029/2006JD007404.

Giorgi, F. (2006a), Regional climate modeling: Status and perspectives, *J. Phys. IV*, *139*, 101–118, doi:10.1051/jp4:2006139008.

Giorgi, F. (2006b), Climate change hot-spots, *Geophys. Res. Lett.*, *33*, L08707, doi:10.1029/2006GL025734.

Giorgi, F., and P. Lionello (2008), Climate change projections for the Mediterranean region, *Global Planet. Change*, *63*, 90–104, doi:10.1016/j.gloplacha.2007.09.005.

Herrera, S., L. Fita, J. Fernández, and J. M. Gutiérrez (2010), Evaluation of the mean and extreme precipitation regimes from the ENSEMBLES regional climate multimodel simulations over Spain, *J. Geophys. Res.*, *115*, D21117, doi:10.1029/2010JD013936.

Herrera, S., J. M. Gutiérrez, R. Ancell, M. Pons, M. D. Frías, and J. Fernández (2012), Development and analysis of a 50-year high-resolution daily gridded precipitation dataset over Spain (Spain02), *Int. J. Climatol.*, *32*, 74–85, doi:10.1002/joc.2256.

Hong, S.-Y., J. Dudhia, and S. Chen (2004), A revised approach to ice microphysical processes for the bulk parameterization of clouds and precipitation, *Mon. Weather Rev.*, *132*(1), 103–120.

Hong, S., V. Lakshmi, E. E. Small, F. Chen, M. Tewari, and K. W. Manning (2009), Effects of vegetation and soil moisture on the simulated land surface processes from the coupled WRF/Noah model, *J. Geophys. Res.*, *114*, D18118, doi:10.1029/2008JD011249.

Intergovernmental Panel on Climate Change (IPCC) (2007), *Climate Change 2007: The Physical Science Basis. Contribution of Working Group I to the Fourth Assessment Report of the Intergovernmental Panel on Climate Change*, edited by S. Solomon et al., Cambridge Univ. Press, Cambridge, U. K.

Janjic, Z. I. (1990), The Step-Mountain Coordinate: Physical package, *Mon. Weather Rev.*, *118*(7), 1429–1443.

Janjic, Z. (1994), The Step-Mountain Eta Coordinate Model: Further developments of the convection, viscous sublayer, and turbulence closure schemes, *Mon. Weather Rev.*, *122*(5), 927–945.

Kjellström, E., F. Boberg, M. Castro, J. Christensen, G. Nikulin, and E. Sánchez (2010), Daily and monthly temperature and precipitation statistics as performance indicators for regional climate models, *Clim. Res.*, *44*(2–3), 135–150.

Laprise, R. (2008), Regional climate modelling, *J. Comput Phys.*, *227*(7), 3641–3666, doi:10.1016/j.jcp.2006.10.024.

Leung, L. R., and Y. Qian (2009), Atmospheric rivers induced heavy precipitation and flooding in the western U.S. simulated by the WRF regional climate model, *Geophys. Res. Lett.*, *36*, L03820, doi:10.1029/2008GL036445.

Liang, X.-Z., K. E. Kunkel, G. A. Meehl, R. G. Jones, and J. X. L. Wang (2008), Regional climate models downscaling analysis of general circulation models present climate biases propagation into future change projections, *Geophys. Res. Lett.*, *35*, L08709, doi:10.1029/2007GL032849.

Pfeiffer, A., and G. Zängl (2010), Validation of climate-mode MM5-simulations for the European Alpine Region, *Theor. Appl. Climatol.*, *101*(1), 93–108.

Pleim, J. E. (2007), A combined local and nonlocal closure model for the atmospheric boundary layer. Part II: Application and evaluation in a mesoscale meteorological mode, *J. Appl. Meteorol. Climatol.*, *46*(9), 1396–1409.

Rodriguez-Puebla, C., A. Encinas, S. Nieto, and J. Garmendia (2008), Spatial and temporal patterns of annual precipitation variability over the Iberian Peninsula, *Int. J. Climatol.*, *18*, 299–316.

Roeckner, E., et al. (2003), The atmospheric general circulation model ECHAM5, *Rep. 349*, Max-Planck-Inst. für Meteorol., Hamburg, Germany.

Rosenberg, E. A., P. W. Keys, D. B. Booth, D. Hartley, J. Burkey, A. C. Steinemann, and D. P. Lettenmaier (2010), Precipitation extremes and the impacts of climate change on stormwater infrastructure in Washington State, *Clim. Change*, *102*, 319–349.

Rummukainen, M. (2010), State-of-the-art with regional climate models, *WIREs Clim. Change*, *1*(1), 82–96.

Salathé, E., Jr., R. Steed, C. F. Mass, and P. H. Wilby (2008), A high-resolution climate model for the U.S. Pacific Northwest: Mesoscale feedbacks and local responses to climate change, *J. Clim.*, *21*, 5708–5726, doi:10.1175/2008JCLI2090.1.

Sánchez, E., C. Gallardo, M. Gaertner, A. Arribas, and M. de Castro (2004), Future climate extreme events in the Mediterranean simulated by a regional climate model: A first approach, *Global Planet. Change*, *44*(1–4), 163–180, doi:10.1016/j.gloplacha.2004.06.010.

Sánchez, E., M. A. Gaertner, C. Gallardo, E. Padorno, A. Arribas, and M. Castro (2007), Impacts of a change in vegetation description on simulated European summer present-day and future climates, *Clim. Dyn.*, *29*(2–3), 319–332,doi:10.1007/s00382-007-0240-2.

Sánchez, E., M. Domínguez, R. Romera, N. López de la Franca, M. Gaertner, C. Gallardo, and M. Castro (2011), Regional modeling of dry spells over the Iberian Peninsula for present climate and climate change conditions, *Clim. Change*, *107*(3–4), 625–634, doi:10.1007/s10584-011-0114-9.

Serrano, A., J. A. García, V. L. Mateos, M. L. Cancillo, and J. Garrido (2008), Monthly modes of variation of precipitation over the Iberian Peninsula, *J. Clim.*, *12*, 2894–2915.

Skamarock, W. C., J. B. Klemp, J. Dudhia, D. O. Gill, D. M. Barker, M. G. Duda, X.-Y. Huang, W. Wang, and J. G. Powers (2008), A description of the Advanced Research WRF version 3, *NCAR Tech. Note, NCAR/TN-475 + STR*, 125pp., Natl. Cent. for Atmos. Res., Boulder, Colo.

Steiner, A., J. Pal, S. Rauscher, J. L. Bergeron, N. Diffenbaugh, A. Boone, L. C. Sloan, and F. Giorgi (2009), Land surface coupling in regional climate simulations of the West African monsoon, *Clim. Dyn.*, *33*(6), 869–892, doi:10.1007/s00382-009-0543-6.

van der Linden, P., and J. F. Mitchell (2009), ENSEMBLES: Climate change and its impacts: Summary of research and results from the ENSEMBLES project, 160 pp., Met Off. Hadley Cent., Exeter, U. K.

von Storch, H., H. Langenberg, and F. Feser (2000), A spectral nudging technique for dynamical downscaling purposes, *Mon. Weather Rev.*, *128*(10), 3664–3673.